waste

MDPI

Article

Recycled Bottle Glass Wastes as Precursors for Porous Alumina Glass Ceramics Synthesis

Cosmin Vancea and Giannin Mosoarca *

Faculty of Industrial Chemistry and Environmental Engineering, Politehnica University Timisoara, Bd. V. Parvan, No. 6, 300223 Timisoara, Romania
* Correspondence: giannin.mosoarca@upt.ro; Tel.: +40-256-404-185

Abstract: This research presents a new solution to use bottle glass wastes together with aluminum hydroxide for porous alumina glass ceramics synthesis. The firing of the samples was conducted at three temperatures: 800, 1000 and 1200 °C. The effect of the bottle waste glass addition on the firing shrinkage, apparent density porosity, chemical stability and compression strength of the sintered samples was investigated. The dimensional stability of the samples, varying between 4.75–11.87% is positively affected by waste glass/alumina substitution ratio. Higher amounts of glass waste lead to higher apparent densities, up to 1.80 g/cm^3 and lower apparent porosities, around 33.74%, depending on the heat treatment temperature. All the studied glass ceramics have very good chemical stability that increase with the glass waste/alumina ratio. The compression strength of the obtained samples, ranging between 4.72–24.20 N/mm^2 is negatively affected by increasing the glass waste amount due to its brittle behavior. The obtained results suggest the viability of the proposed recycling alternative for bottle glass waste together with aluminum hydroxide as porous alumina glass ceramics.

Keywords: glass waste; porous alumina; glass ceramics

Citation: Vancea, C.; Mosoarca, G. Recycled Bottle Glass Wastes as Precursors for Porous Alumina Glass Ceramics Synthesis. *Waste* **2023**, *1*, 115–126. https://doi.org/10.3390/waste1010009

Academic Editor: Christopher Cheeseman

Received: 30 September 2022
Revised: 23 November 2022
Accepted: 1 December 2022
Published: 3 December 2022

1. Introduction

The world population growth generates an increase demand for goods and leads to a large amount of disposable waste [1]. Apart from the environmental problems related to proper disposal at landfill sites, increasing cost for land disposal for those residues and their appropriate treatment avoiding soil and water contamination, the depletion of natural resources must be considered [2,3].

Glass recycling leads to some important benefits for the glass industry, that use glass pellets as substitute for raw materials, thus reducing the raw materials extraction, energy consumption, waste reduction in landfills and CO_2 emissions [4].

Huge quantities of glass wastes are produced worldwide, but only small amounts are redirected into recycling with majority ending at stockpiles [5]. Compared with other types of solid waste, glass is chemically stable and nonbiodegradable over a long period of time [6]. Theoretically, glass is 100% recyclable, it can be indefinitely recycled without significant loss of quality. However, the contamination in recycling bins and the difficulty to sort mixed color waste glass makes the recycling process impractical [7].

Glass waste recycling can be economically viable only by manufacturing new marketable products. The civil and construction industries use recycled glass as aggregates for architectural concrete [8–10], pavements [11] and road construction material [12]. New glass ceramic materials having good thermal, mechanical, chemical, biological and dielectric properties can be synthesized using recycled glass [13–15]. The glass powder obtained by mechanical crushing can replace the sodium silicate in manufacturing geopolymers, based on its' high amount of silica [16,17]. Glass fibers recycled into reinforced materials can be achieved by mixing with various materials as cements [18], gypsum [19], alkali [20] and carbon fibers [21]. Foamed glass is a lightweight insulator synthesized through a specific heat treatment using a mix of recycled glass powder together with various foaming agents. The structure of the obtained porous material consists of sealed glass cells that prevent the movement of moisture [22,23].

Porous alumina ceramics are known for their high porosity and high specific surface area, high thermal resistance and chemical stability towards corrosive environments [24–27]. These materials have a wide application range as biomedical implants [28], hot-gas purifiers [29], molten metal filtration [30] and thermal insulation [31]. The large number of waste materials used as foaming agents used can be grouped into two categories: agricultural and industrial waste materials [32].

Current techniques for porous alumina ceramics mentioned in the literature use for ceramic synthesis the organic foam, the freeze-casting, sol-gel, the partial sintering and pore-forming agent methods [32]. Fabrication of porous ceramics using the pore-forming method is widely used for different kind of ceramic bodies. Dedicated foaming agents such as SiC, carbonates, sulphates and various waste materials are mentioned by other authors [33–35].

This research suggests a new alternative to obtain porous alumina glass ceramics using recycled bottle glass together with aluminum hydroxide that functions both as source of Al_2O_3 and as foaming agent.

2. Materials and Methods

The bottle glass waste used in this study was supplied by the municipal waste management and disposal service of the city of Timisoara. The glass chemical composition, determined by RX fluorescence using a Niton XL 3 equipment (Thermo Fisher Scientific Inc., Waltham, MA, USA), is shown in Table 1. The glass waste powder that resulted after grinding in a Pulverisette type laboratory mill (Fritsch GmbH, Idar-Oberstein, Germany) using a material:balls:water ratio of 1:2:1 was dried in an oven at 105 °C for 24 h and then sieved, the granulometric fraction under 100 μm mesh being retained for later use.

Table 1. The bottle glass waste oxidic composition (weight %).

Oxide	SiO_2	Na_2O	K_2O	CaO	MgO	Al_2O_3	Fe_2O_3
Quantity	74.42	12.90	0.19	11.27	0.46	0.75	0.01

The aluminum hydroxide, provided by SC ALUM SA Tulcea (Tulcea, Romania) contains >99.5% $Al(OH)_3$ and is characterized by a specific surface area of 4.6 $m^2 \cdot g^{-1}$ and a picnometric density of 2.41 $g \cdot cm^{-3}$ and particle size (D_{50}) of 0.94 μm.

The batch recipes used in the glass ceramics synthesis are illustrated in Table 2.

Table 2. Batch recipes (weight %) for the glass ceramics synthesis.

Sample	Glass Waste (%)	Al_2O_3 (%)
1	50.00	50.00
2	33.33	66.67
3	25.00	75.00
4	20.00	80.00
5	16.67	83.33
6	14.29	85.71
7	12.50	87.50
8	11.11	88.89
9	10.00	90.00
10	9.09	90.91

The appropriate amount of $Al(OH)_3$ was calculated for each recipe based on the specific decomposition chemical reaction:

$$2\,Al(OH)_3 \rightarrow Al_2O_3 + 3\,H_2O$$

The precursors were mixed together and pressed into cylindrical shapes using a BERNARDO WK 10 TH hydraulic press (PWA HandelsgesmbH, Linz, Austria). The firing process was conducted considering a heating rate of 10 °C·min^{-1} in the temperature range 20–650 °C and 30 °C·min^{-1} from 650 °C up to the peak firing temperatures: 800, 1000 and 1200 °C that were maintained for 120 min in a Nabertherm 300–1300 °C electric furnace (Nabertherm GmbH, Lilienthal, Germany). In order to avoid thermal stress, the samples were annealed for 4 h at 550 °C and then slowly cooled to room temperature.

The obtained samples' dimensional stability was determined based on the volumetric shrinkage after firing, measured with an electronic caliper.

The apparent density and apparent porosity of the synthesized glass ceramics were measured at 20 °C using the liquid saturation method under vacuum with water as the working liquid.

The total porosity of the studied samples was calculated using the relation:

$$P = \left(1 - \frac{\rho_S}{\rho_P}\right) \cdot 100\ (\%) \tag{1}$$

where $\rho_S = \frac{m_S}{V_S}$ (g·cm^{-3}) is the bulk density of the cylindrical shape sample and ρ_P is the material density, determined by pycnometer method using demineralized water as the working liquid at 20 °C.

The microporous structure of the glass–ceramic matrices was analyzed by SEM, using a Quanta FEG 250 microscope (FEI Company, Hillsboro, OR, USA) using the low vacuum mode at 20.0 kV.

The phase compositions of synthesized glass ceramics were studied with a Rigaku Ultima 4 diffractometer (Rigaku Corp.,Tokyo, Japan) using the monochromatic Cu-K radiation. The XRD patterns were recorded using an angular range of 5° to 80° for a scanning speed of 20°/min at every 0.05 interval. XRD analyses were conducted using PDXL software (Rigaku Corp.,Tokyo, Japan), for the phase identification were used PDF (Powder Diffraction File, PDF 2) cards, by the Joint Committee on Powder Diffraction Standards (JCPDS) and the International Centre for Diffraction Data (ICDD).

The chemical stability of the obtained glass ceramics was determined considering their dissolution rate (Dr) in deionized water. The samples having an initial measured mass mi, were immersed for 28 days in 100 mL deionized water maintained at a temperature of 20 °C and then dried until reaching constant mf mass in a laboratory oven at 110 °C. The dissolution rate (Dr) was calculated based on the relation:

$$Dr = \Delta m / t\ (\mu g/h) \tag{2}$$

where $\Delta m = m_i - m_f$ is the weight loss leached by deionized water after the time t.

The compression tests were conducted for all the obtained samples using a Zwick Roell AllroundLine equipment (ZwickRoell Testing Systems GmbH., Fürstenfeld, Austria) using a 5–250 kN test load cell and a crosshead speed of 1.0 mm/min. The synthesized cylindrical shape samples were polished to obtain highly parallel and smooth opposite bases surfaces. The specimen geometries described by the length/diameter range 1.5–2.5, recommended by ASTM C1424-15(2019), were verified for each tested sample.

3. Results and Discussion

3.1. Dimensional Deviations after Firing

The firing shrinkage of the studied samples occurs due to the structural changes that affect the glass ceramic matrix at high temperature. The volume contractions of the samples are presented in Figure 1 for the three considered firing temperatures.

The volume shrinkage ranges from 4.75–10.1% for the samples fired at 800 °C up to 6.55–11.87% for those obtained at 1200 °C. As the heat treatment temperature increases, the amount and fluidity of the glass melt increases accordingly, leading to higher dimensional deviations.

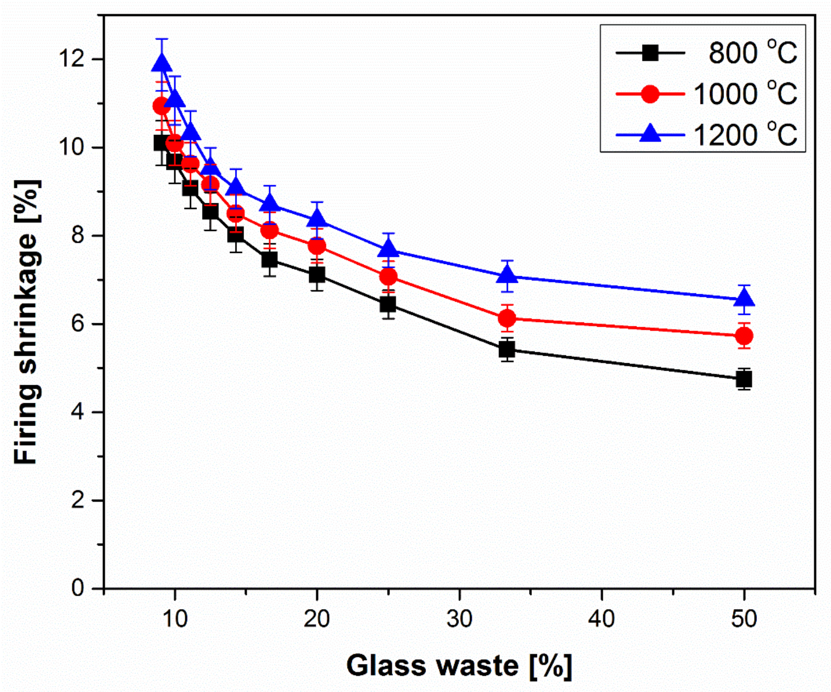

Figure 1. Evolution of firing shrinkage vs. glass waste amount.

The substitution of the glass waste precursor with Al_2O_3 leads to higher dimensional deviations in the obtained samples due to lower amounts of the vitreous phase generated during the firing process, an effect that becomes more important as the firing temperature increases.

3.2. Apparent Densities, Total and Apparent Porosities of the Glass Ceramics

The influence of the glass waste amount upon the apparent density and the total and apparent porosity of the obtained glass ceramic are illustrated in Figures 2 and 3.

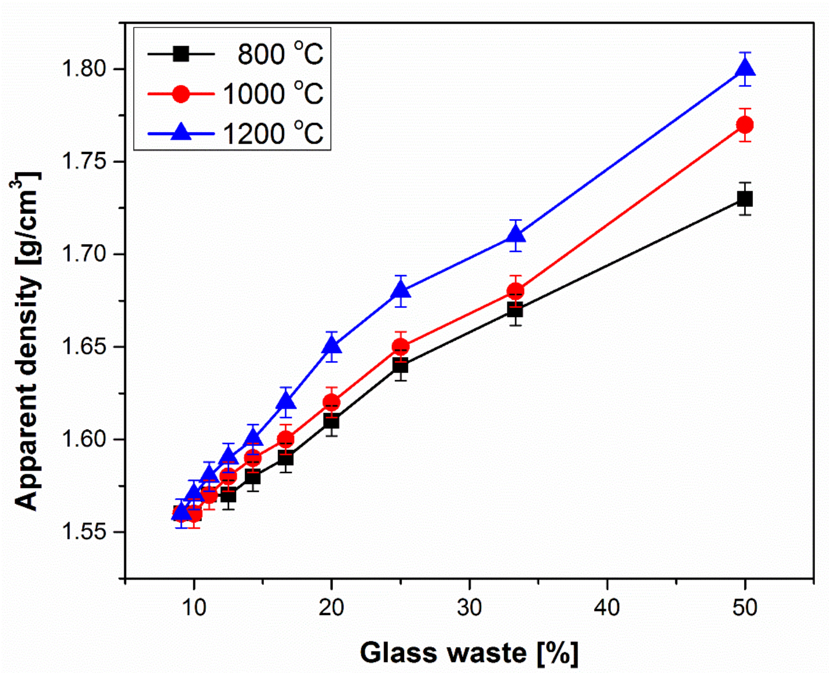

Figure 2. Influence of the glass waste amount upon the apparent density of the studied samples.

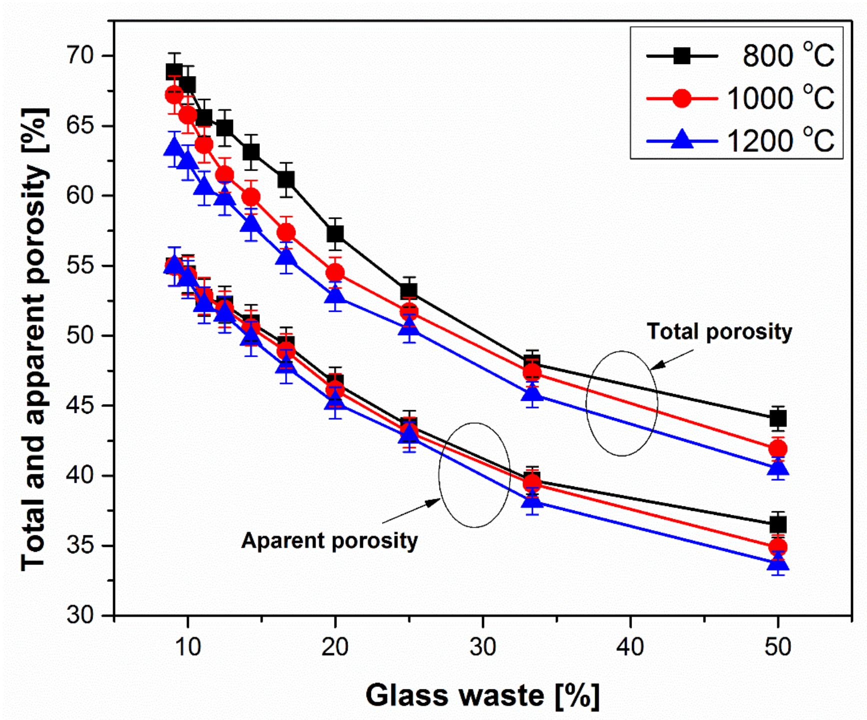

Figure 3. Influence of the glass waste amount upon the total and apparent porosity of the studied samples.

The values of the apparent density of the obtained glass ceramics increase from 1.56–1.73 g/cm^3 at 800 °C up to 1.56–1.80 g/cm^3 at 1200 °C while the samples' apparent porosities decrease from 36.49–54.96% down to 33.74–54.94% for the same firing temperatures. This behavior is generated by the larger amounts of liquid phase generated as the heat treatment temperature increases, which is able to fill the glass ceramic matrix pores, leading to lower porosities and higher densities.

As the glass waste amount used for sample synthesis decreases, the apparent porosities increase and the apparent densities decrease accordingly, due to the lower quantities of vitreous melt generated at the firing temperature able to fill the available structural pores.

The total porosity of the studied samples follows a similar evolution to that of the apparent porosity both with the firing temperature and with the amount of waste glass used for the synthesis. The increase of the heat treatment temperature leads to a decrease from 44.08–68.81% at 800 °C to 40.53–63.34% at 1200 °C. The contribution of the open pores to the total porosity of the obtained glass ceramics, calculated as a percentage is illustrated in Table 3.

Table 3. Open cell contribution to the glass ceramic total porosity.

Sample	Glass Waste	P_{ap}/P_{total} [%]		
		800 °C	1000 °C	1200 °C
1	50	82.77	83.25	83.26
2	33.33	82.64	83.30	83.33
3	25	81.97	83.36	84.67
4	20	81.40	84.59	85.61
5	16.67	80.73	85.23	86.01
6	14.29	80.69	84.40	85.94
7	12.5	80.55	84.39	86.10
8	11.11	80.40	82.99	86.17
9	10	80.11	82.53	86.60
10	9.09	79.87	81.75	86.74

The majority of the porous structure of the studied materials is based on open cells, their total contribution ranging from 79.87 to 86.74% of total porosity, values comparable to those obtained by other researchers [36,37].

The porous microstructure of two of the studied samples are presented in Figure 4: sample 1 containing 50% glass waste and sample 10 containing 10% glass waste.

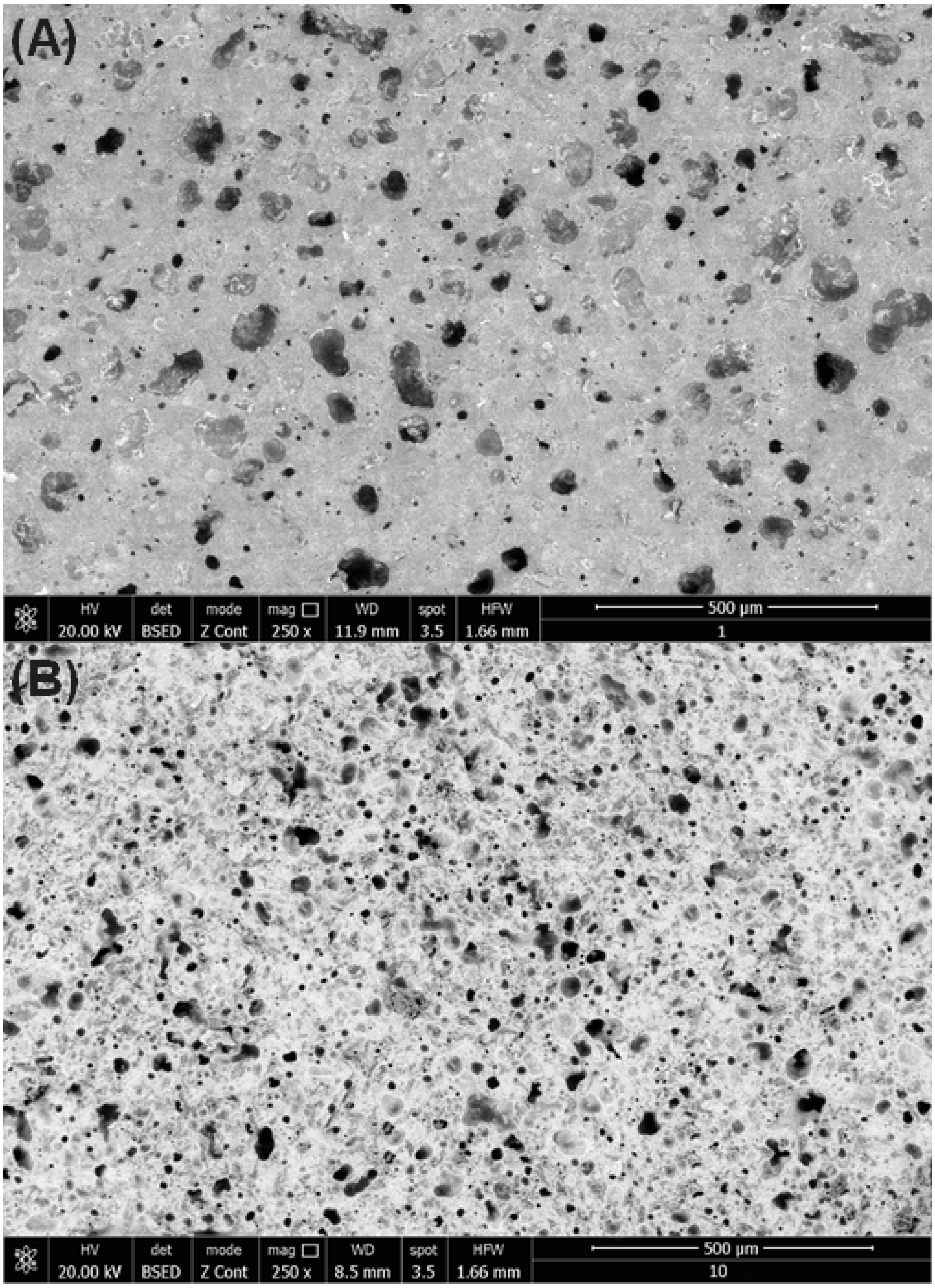

Figure 4. Porous microstructure of samples 1 (**A**) and 10 (**B**).

The SEM images illustrate the effect of the glass waste amount on the pores size and distribution. Sample 1, containing 50% glass waste has relatively few large pores, formed by coalescence of smaller pores, favored by the liquid phase generated by the glass melt, unevenly distributed on the surface of the sample. A much lower amount of glass waste used to synthesize sample 10 leads to a different morphology of the porous structure that contains a larger number of small pores relatively evenly distributed on the surface.

3.3. Phase Composition

The XRD pattern for sample 1, containing 50% glass waste, after the firing process at 800 °C and 1200 °C is presented in Figure 5.

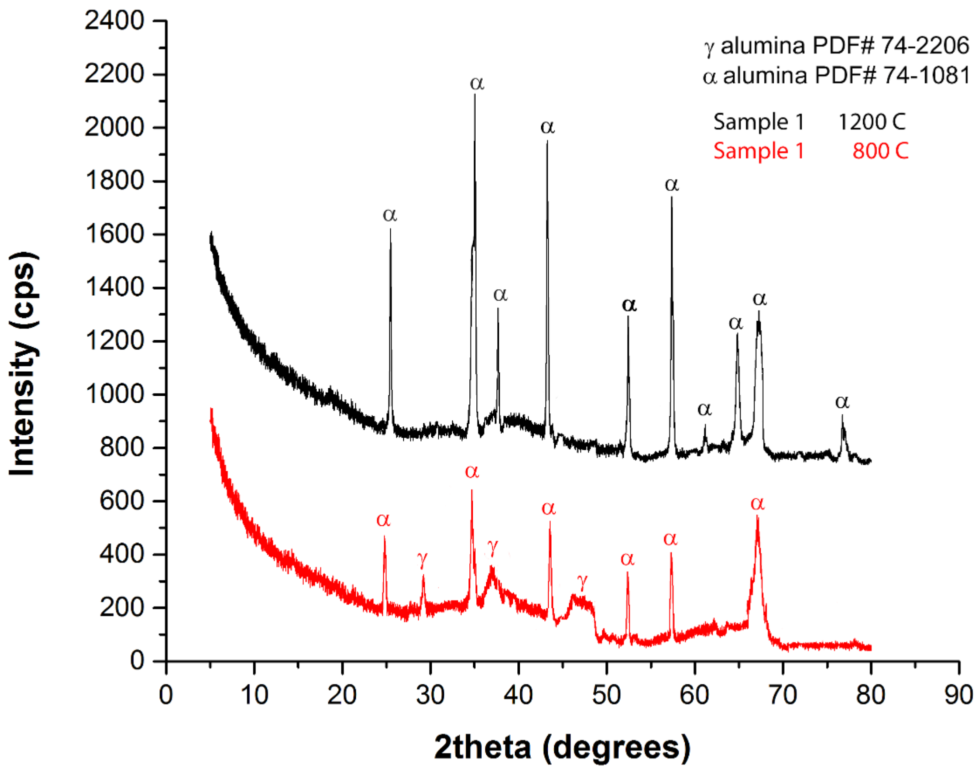

Figure 5. Phase composition of samples 1 heat treated at 800 °C and 1200 °C.

The XRD patterns indicate the presence of α alumina (PDF# 74-1081) and γ-alumina (PDF# 74-2206) for the glass ceramic fired at 800 °C, that have a relative low crystallinity, as illustrated by the halo between 34–45° [38]. The sample fired at 1200 °C shows sharper peaks, indicating a higher crystallinity, the dominant phase being α alumina (PDF# 74-1081) [39]. The broad shape of both patterns for lower angular range is specific for the amorphous vitreous phase present in the glass ceramic structure [40].

3.4. Chemical Stability of the Samples

The effect of the glass waste amount used in the synthesis process upon the chemical stability expressed as dissolution rate after 28 days is illustrated in Figure 6.

All the synthesized glass ceramics have a very good chemical stability, their dissolution rates ranging between 0.018–0.069 µg/h when firing at 800 °C to 0.010–0.06 µg/h when the heat treatment was conducted at 1200 °C. Using higher amounts of glass waste has a favorable effect upon the samples' chemical stability due to the fact that the vitreous phase generated has a superior hydrolytic stability compared to the alumina ceramic phase.

3.5. Mechanical Properties of the Glass Ceramics

The target applications of obtained glass ceramics as supports for catalysts, refractory bricks or filters for molten metals implies good compressive strength. The effect of the glass waste upon the compression strength of the obtained samples is shown in Figure 7.

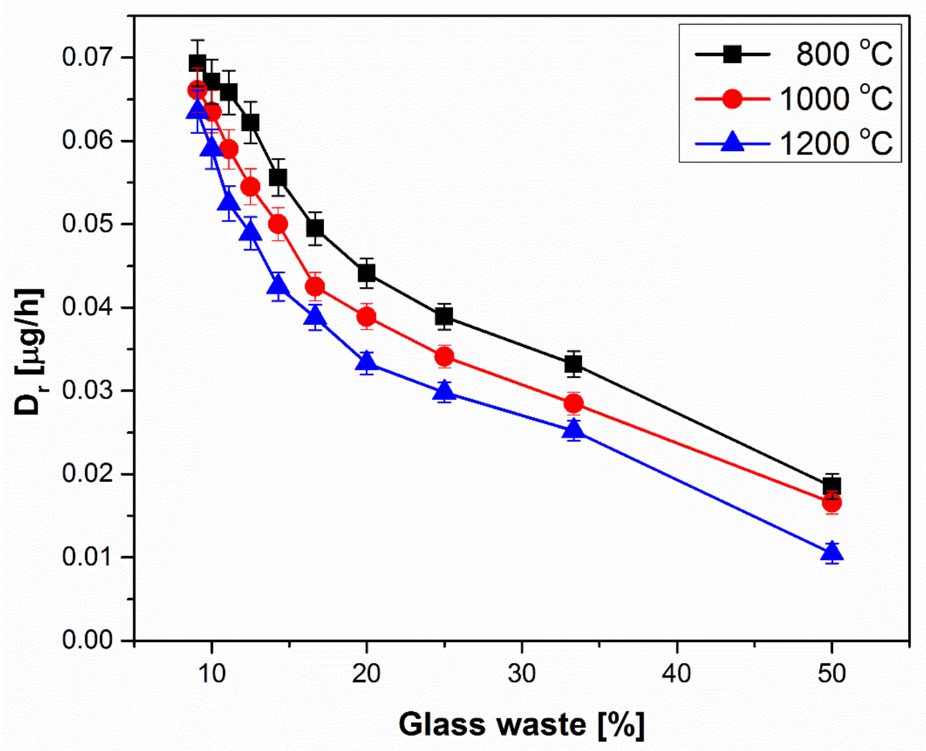

Figure 6. Influence of the glass waste amount upon the studied samples dissolution rate.

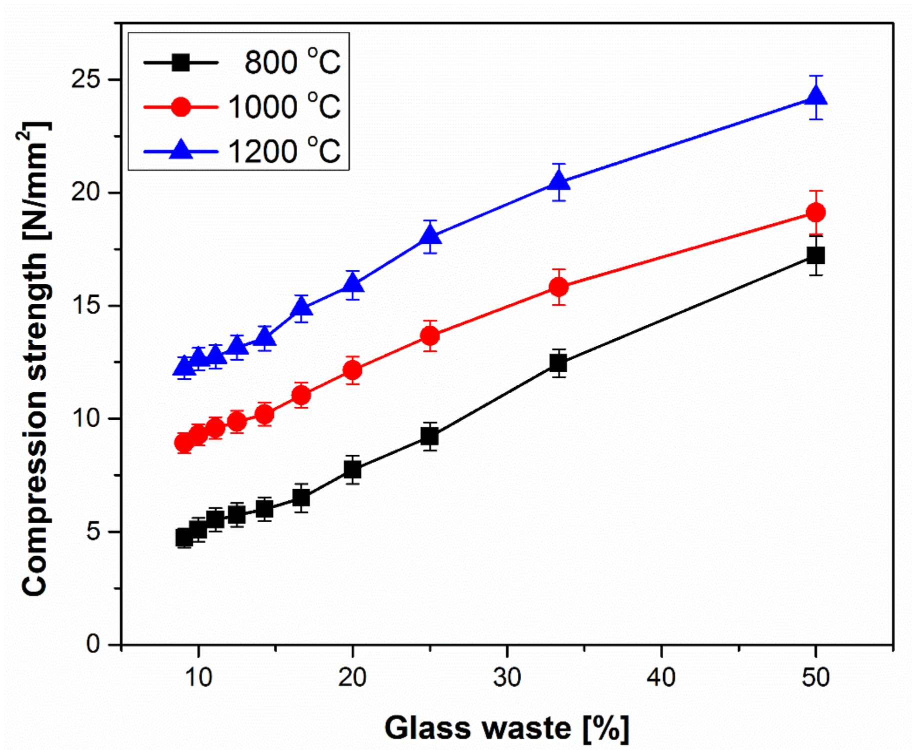

Figure 7. Influence of the glass waste amount upon the studied samples compression strength.

The compression strength of the samples obtained at 800 °C, ranging between 4.72–17.21 N/mm^2 is lower compared to that obtained after sintering at 1200 °C, ranging between 12.24–24.20 N/mm^2. The main contribution to the mechanical strength of the samples is due to the ceramic alumina bonds, formed at higher firing temperature.

The effect of the glass waste amount used for the samples synthesis upon the compression strength can be discussed considering the apparent porosity as presented in Figure 8.

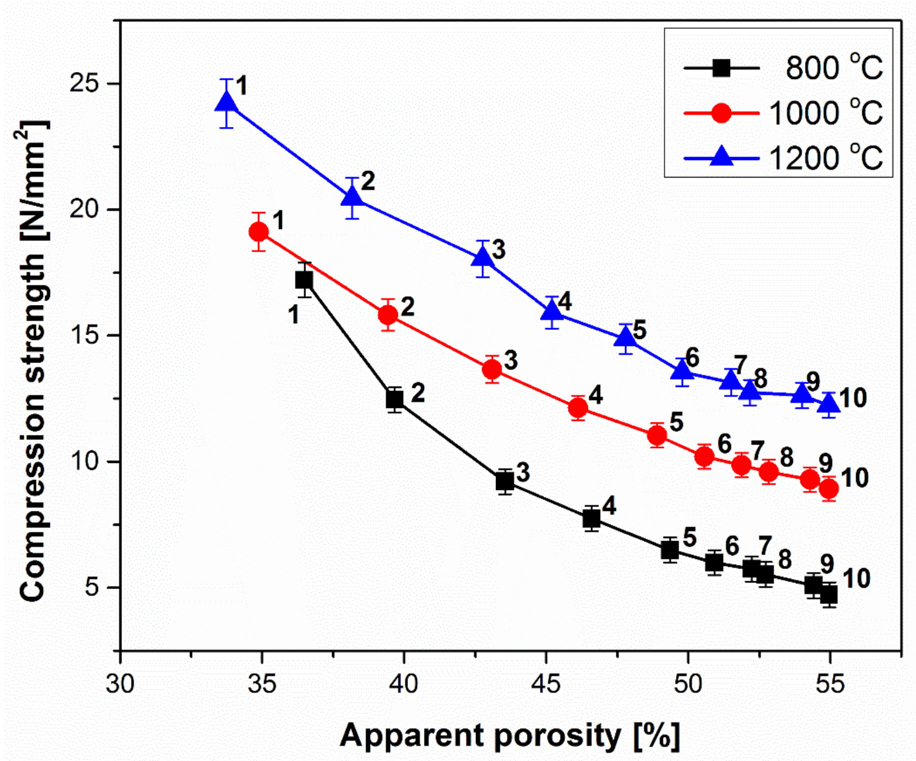

Figure 8. Influence of the sample's apparent porosity upon compression strength.

As the glass waste amount increases, the liquid phase formed at the firing temperature fills the pores leading to a less fragmented structure of the glass ceramic matrix. The decrease of the structural discontinuities generated by pores leads to an increase of the compression strength of the samples accordingly.

The obtained values were compared with the literature data for porous aluminum materials in the Table 4.

Table 4. Comparison of the obtained samples compression strength with other porous alumina ceramics mentioned in the literature.

Apparent Porosity (%)	Compression Strength (N/mm^2)	Reference
35.0–54.0	57.4–17.7	[19]
59.0–82.0	95.0–11.0	[20]
61.9	3.01	[21]
33.7–54.9	4.72–24.20	Actual study

The values of the compression strength of the researched glass ceramics are comparable to the results obtained by other researchers. When comparing previous data, it should be taken into account that some authors tested sintered materials fired at temperatures above 1600 °C, much higher than the firing temperature used in this study. This fact favors the development of the crystalline structure of alumina, and implicitly, the development of higher mechanical resistances.

4. Conclusions

A new alternative of using bottle glass wastes together with aluminum hydroxide to obtain porous alumina glass ceramics was proposed. The main advantage of this method is that the aluminum hydroxide functions both as source of Al_2O_3 and as foaming agent.

The dimensional stability of the synthesized glass ceramics, ranging between 4.75–11.87% is positively affected by waste glass/alumina substitution ratio. The increase of the firing temperature leads to higher dimensional deviations due to the higher amount and fluidity of the glass melt generated.

The apparent density varies between 1.56–1.73 g/cm^3 after firing at 800 °C, up to 1.56–1.80 g/cm^3 when using a temperature of 1200 °C. The apparent porosity ranges from 36.49–54.96% to 33.74–54.94% for the same firing temperatures. Increasing the heat treatment temperature affects the porosity of the samples by generating larger amounts of liquid phase able to fill the glass ceramic matrix pores. Using higher amounts of glass waste leads to higher apparent densities and lower apparent porosities due to the higher quantities of vitreous melt generated at the firing temperature able to fill the available structural pores.

The porous structures of the obtained glass ceramics were characterized by measuring the contribution of the open cells to the total porosity, their total contribution ranging from 79.87% to 86.74% of the total porosity. The SEM analysis confirms the effect of the glass waste amount on the pore size and distribution, based on the behavior of the melted glass, which is able to fill the available pores and to generate the coalescence of the unfilled pores through the fluid medium.

The obtained values of the dissolution rate ranging between 0.010 and 1.069 µg/h confirmed the very good chemical stability of the sintered alumina glass ceramics. Using higher firing temperatures and larger amounts of glass waste have a positive effect upon the samples' chemical stability knowing that the vitreous phase has a superior hydrolytic stability compared to the ceramic phase.

The compression strength of the obtained samples, varying between 4.72 and 24.20 N/mm^2 is positively affected by the heat treatment temperature, which favors the formation of alumina ceramic bonds, resistant to mechanical stress. Higher glass waste amounts used for samples synthesis leads to lower porosities and therefore less fragmented glass ceramic matrices and higher compression strength of the samples.

The obtained results highlight the viability of the suggested solution to use bottle glass wastes together with aluminum hydroxide for porous alumina glass ceramic synthesis.

Author Contributions: Conceptualization, C.V. and G.M.; methodology, C.V. and G.M.; software, C.V.; validation, C.V. and G.M.; formal analysis, C.V. and G.M.; investigation, C.V. and G.M.; resources, C.V.; data curation, C.V. and G.M.; writing—original draft preparation, C.V. and G.M.; writing—review and editing, C.V. and G.M.; visualization, C.V.; supervision, C.V. All authors have read and agreed to the published version of the manuscript.

Funding: This research received no external funding.

Institutional Review Board Statement: Not applicable.

Informed Consent Statement: Not applicable.

Data Availability Statement: All the experimental data obtained are presented, in the form of table and/or figure, in the article.

Conflicts of Interest: The authors declare no conflict of interest.

References

1. da Silva, R.C.; Puglieri, F.N.; de Genaro Chiroli, D.M.; Bartmeyer, G.A.; Kubaski, E.T.; Tebcherani, S.M. Recycling of glass waste into foam glass boards: A comparison of cradle-to-gate life cycles of boards with different foaming agents. *Sci. Total Environ.* **2021**, *771*, 145276. [CrossRef] [PubMed]
2. Wang, X.; Feng, D.; Zhang, B.; Li, Z.; Li, C.; Zhu, Y. Effect of KNO_3 on the microstruture and physical properties of glass foam from solid waste glass and SiC powder. *Mater. Lett.* **2016**, *169*, 21–23. [CrossRef]
3. Samadi, M.; Huseien, G.F.; Mohammadhosseini, H.; Lee, H.S.; Abdul Shukor Lim, N.H.; Tahir, M.M.d.; Alyousef, R. Waste ceramic as low cost and eco-friendly materials in the production of sustainable mortars. *J. Clean. Prod.* **2020**, *266*, 121825. [CrossRef]
4. García Guerrero, J.; Rodríguez Reséndiz, J.; Rodríguez Reséndiz, H.; Álvarez-Alvarado, J.M.; Rodríguez Abreo, O. Sustainable Glass Recycling Culture-Based on Semi-Automatic Glass Bottle Cutter Prototype. *Sustainability* **2021**, *13*, 6405. [CrossRef]
5. Robert, D.; Baez, E.; Setunge, S. A new technology of transforming recycled glass waste to construction components. *Constr. Build. Mater.* **2021**, *313*, 125539. [CrossRef]

6. Guo, P.; Meng, W.; Nassif, H.; Gou, H.; Bao, Y. New perspectives on recycling waste glass in manufacturing concrete for sustainable civil infrastructure. *Constr. Build. Mater.* **2020**, *257*, 119579. [CrossRef]
7. Danguolė, B.; Dagnija, B.; Saulius, V.; Gintautas, S. Multicriteria analysis of glass waste application. *Environ. Clim. Technol.* **2019**, *23*, 152–167.
8. Kechagia, P.; Koutroumpi, D.; Bartzas, G.; Peppas, A.; Samouhos, M.; Deligiannis, S.; Tsakiridis, P.E. Waste marble dust and recycled glass valorization in the production of ternary blended cements. *Sci. Total Environ.* **2021**, *761*, 143224. [CrossRef]
9. Ferdous, W.; Manalo, A.; Siddique, R.; Mendis, P.; Zhuge, Y.; Wong, H.S.; Lokuge, W.; Aravinthan, T.; Schubel, P. Recycling of landfill wastes (tyres, plastics and glass) in construction—A review on global waste generation, performance, application and future opportunities. *Resour. Conserv. Recycl.* **2021**, *173*, 105745. [CrossRef]
10. Ogundairo, T.O.; Adegoke, D.D.; Akinwumi, I.I.; Olofinnade, O.M. Sustainable use of recycled waste glass as an alternative material for building construction—A review. *IOP Conf. Series: Mater. Sci. Eng.* **2019**, *640*, 012073. [CrossRef]
11. Perera, S.T.A.M.; Zhu, J.; Saberian, M.; Liu, M.; Cameron, D.; Maqsood, T.; Li, J. Application of Glass in Subsurface Pavement Layers: A Comprehensive Review. *Sustainability* **2021**, *13*, 11825. [CrossRef]
12. Poulikakos, L.D.; Papadaskalopoulou, C.; Hofko, B.; Gschösser, F.; Cannone Falchetto, A.; Bueno, M.; Arraigada, M.; Sousa, J.; Ruiz, R.; Petit, C.; et al. Harvesting the unexplored potential of European waste materials for road construction. *Resour. Conserv. Recycl.* **2017**, *116*, 32–44. [CrossRef]
13. Zhang, Z.; Li, Z.; Yang, Y.; Shen, B.; Ma, J.; Liu, L. Preparation and characterization of fully waste-based glass-ceramics from incineration fly ash, waste glass and coal fly ash. *Ceram. Int.* **2022**, *48*, 21679–21688. [CrossRef]
14. Hanning, E.; Gualberto, H.R.; Simões, K.M.A.; Bertolino, L.C.; Poiate, E.; Andrade, M.C. Glass-ceramic produced with recycled glass. *Matéria* **2019**, *24*, 12505. [CrossRef]
15. Silva, R.V.; de Brito, J.; Lye, C.Q.; Dhir, R.K. The role of glass waste in the production of ceramic-based products and other applications: A review. *J. Clean. Prod.* **2017**, *167*, 346–364. [CrossRef]
16. Bilondi, M.P.; Toufigh, M.M.; Toufigh, V. Experimental investigation of using a recycled glass powder-based geopolymer to improve the mechanical behavior of clay soils. *Constr. Build. Mater.* **2018**, *170*, 302–313. [CrossRef]
17. Luhar, S.; Cheng, T.W.; Nicolaides, D.; Luhar, I.; Panias, D.; Sakkas, K. Valorisation of glass wastes for the development of geopolymer composites—Durability, thermal and microstructural properties: A review. *Constr. Build. Mater.* **2019**, *222*, 673–687. [CrossRef]
18. Chang, J.-H.; Tsai, Y.-S.; Yang, P.-Y. A Review of Glass Fibre Recycling Technology Using Chemical and Mechanical Separation of Surface Sizing Agents. *Recycling* **2021**, *6*, 79. [CrossRef]
19. Gonçalves, R.M.; Martinho, A.; Oliveira, J.P. Evaluating the potential use of recycled glass fibers for the development of gypsum-based composites. *Constr. Build. Mater.* **2022**, *321*, 126320. [CrossRef]
20. Mokhtar, M.; Kraxner, I.; Kaňková, H.; Hujová, M.; Chen, S.; Galusek, D.; Bernardo, E. Porous glass microspheres from alkali-activated fiber glass waste. *Materials* **2022**, *15*, 1043.
21. Karuppannan Gopalraj, S.; Kärki, T. A review on the recycling of waste carbon fibre/glass fibre-reinforced composites: Fibre recovery, properties and life-cycle analysis. *SN Appl. Sci.* **2020**, *2*, 433. [CrossRef]
22. Owoeye, S.S.; Matthew, G.O.; Ovienmhanda, F.O.; Tunmilayo, S.O. Preparation and characterization of foam glass from waste container glasses and water glass for application in thermal insulations. *Ceram. Int.* **2020**, *46*, 11770–11775. [CrossRef]
23. Siddika, A.; Hajimohammadi, A.; Sahajwalla, V. Powder sintering and gel casting methods in making glass foam using waste glass: A review on parameters, performance, and challenges. *Ceram. Int.* **2022**, *48*, 1494–1511. [CrossRef]
24. Jean, G.; Sciamanna, V.; Demuynck, M.; Cambier, F.; Gonon, M. Macroporous ceramics: Novel route using partial sintering of alumina-powder agglomerates obtained by spray-drying. *Ceram. Int.* **2014**, *40*, 10197–10203. [CrossRef]
25. da Costa, F.P.; da Silva Morais, C.R.; Pinto, H.C.; Rodrigues, A.M. Microstructure and physico-mechanical properties of Al_2O_3-doped sustainable glass-ceramic foams. *Mater. Chem. Phys.* **2020**, *256*, 123612. [CrossRef]
26. Alzukaimi, J.; Jabrah, R. The preparation and characterization of porous alumina ceramics using an eco-friendly pore-forming agent. *Int. J. Appl. Ceram.* **2018**, *16*, 820–831. [CrossRef]
27. Geng, H.; Hu, X.; Zhou, J.; Xu, X.; Wang, M.; Guo, A.; Du, H.; Liu, J. Fabrication and compressive properties of closed-cell alumina ceramics by binding hollow alumina spheres with high-temperature binder. *Ceram. Int.* **2016**, *42*, 16071–16076. [CrossRef]
28. Yoon, B.H.; Choi, W.Y.; Kim, H.E.; Kim, J.H.; Koh, Y.H. Aligned porous alumina ceramics with high compressive strengths for bone tissue engineering. *Scr. Mater.* **2008**, *58*, 537–540. [CrossRef]
29. Ciurans Oset, M.; Nordin, J.; Akhtar, F. Processing of Macroporous Alumina Ceramics Using Pre-Expanded Polymer Microspheres as Sacrificial Template. *Ceramics* **2018**, *1*, 329–342. [CrossRef]
30. Kennedy, M.W.; Zhang, K. Characterization of ceramic foam filters used for liquid metal filtration. *Metall. Mater. Trans. B* **2013**, *44*, 671–690. [CrossRef]
31. Wang, Z.; Feng, P. Porous mullite thermal insulators from coal gangue fabricated by a starch-based foam gel-casting method. *J. Aust. Ceram. Soc.* **2017**, *53*, 287–291. [CrossRef]
32. Ali, M.S.; Hanim, M.A.A.; Tahir, S.M.; Jaafar, C.N.A.; Norkhairunnisa, M.; Matori, K.A. Preparation and characterization of porous alumina ceramics using different pore agents. *J. Ceram. Soc. Jpn.* **2017**, *125*, 402–412. [CrossRef]
33. Dong, Y.; Hampshire, S.; Zhou, J.; Lin, B.; Ji, Z.; Zhang, X.; Meng, G. Recycling of fly ash for preparing porous mullite membrane supports with titania addition. *J. Hazard. Mater.* **2010**, *180*, 173–180. [CrossRef] [PubMed]

34. Mohanta, K.; Kumar, A.; Parkash, O.; Kumar, D. Processing and properties of low cost macroporous alumina ceramics with tailored porosity and pore size fabricated using rice husk and sucrose. *J. Eur. Ceram. Soc.* **2014**, *34*, 2401–2412. [CrossRef]
35. Sengphet, K.; Pasomsouk, K.; Sato, T.; Fauzi, M.A.; Radzali, O.; Pinang, S.P. Fabrication of Porous Clay Ceramics Using Kenaf. Powder Waste. *Int. J. Sci. Res. Publ.* **2013**, *3*, 1–5.
36. Wang, L.; An, L.; Zhao, J.; Shimai, S.; Mao, X.; Zhang, J.; Liu, J.; Wang, S. High-strength porous alumina ceramics prepared from stable wet foams. *J. Adv. Ceram.* **2021**, *10*, 852–859. [CrossRef]
37. Tang, X.; Zhang, Z.; Zhang, X.; Huo, W.; Liu, J.; Yan, S.; Yang, J. Design and formulation of polyurethane foam used for porous alumina ceramics. *J. Polym. Res.* **2018**, *25*, 136. [CrossRef]
38. Rogojan, R.; Andronescu, E.; Ghitulica, C.; Vasile, B. Synthesis and characterization of alumina nano-powder obtained by sol-gel method. *UPB Sci. Bull. B Chem. Mater. Sci.* **2011**, *73*, 67–76.
39. Lu, X.; Yang, J.; Li, X.; Sun, F.; Wang, F.; Chao, Y. Effects of phase transformation on properties of alumina ceramic membrane: A new assessment based on quantitative X-ray diffraction (QXRD). *Chem. Eng. Sci.* **2019**, *199*, 349–358. [CrossRef]
40. Krstić, I.; Zec, S.; Lazarević, V.; Stanisavljević, M.; Golubović, T. Use of sintering to immobilize toxic metals present in galvanic sludge into a stabile glass-ceramic structure. *Sci. Sinter.* **2018**, *50*, 139–147. [CrossRef]